

Three Agulhas rings observed during the Benguela Current Experiment

Silvia L. Garzoli,¹ Philip L. Richardson,² Christopher M. Duncombe Rae,³
David M. Fratantoni,² Gustavo J. Goñi,¹ and Andreas J. Roubicek¹

Abstract. A field program to study the circulation of the Benguela Current and its extension into the southeastern Atlantic Ocean has completed the survey and instrument deployment phase. We report here new observations of three Agulhas rings north and west of Cape Town, South Africa. Three mesoscale anticyclonic rings initially identified by means of TOPEX/POSEIDON altimetry were surveyed with expendable bathythermographs, conductivity-temperature-depth-oxygen profiles, direct current measurements from a lowered acoustic Doppler current profiler, a hull-mounted acoustic Doppler current profiler, and satellite-tracked surface drifters. Characteristics of the rings are presented, and their origins are discussed. Two are typical Agulhas rings surveyed at different times after their generation; the third Agulhas ring has an anomalous water mass structure whose most likely origin is the Subtropical Front.

1. Introduction

The South Atlantic Ocean is a major conduit for warm upper layer water that flows northward across the equator in compensation for the colder southward flowing North Atlantic Deep Water. *Gordon et al.* [1992] concluded that the major proportion of deep water exported from the North Atlantic is balanced by northward flow of lower thermocline and intermediate water through the South Atlantic Ocean. This large-scale thermohaline circulation, the so-called conveyor belt [*Broecker, 1991*], is responsible for the northward heat flux through the South Atlantic. Within the subtropical region the northward heat flux estimates range from 0.5–1.3 PW [*Peterson and Stramma, 1991; Saunders and King, 1995*].

The Benguela Current is a broad, northward flow adjacent to southwestern Africa that forms the eastern limb of the South Atlantic Subtropical Gyre. At 30°S the entire current is confined between the African coast and the Walvis Ridge near the Greenwich meridian. The Benguela Current has two primary sources of water, the South Atlantic Current and Indian Ocean Water that rounds the southern tip of Africa via the Agulhas Current [*Gordon et al., 1992*].

Indian Ocean Water enters the South Atlantic by both a ring-shedding process at the western end of the Agulhas Retroreflection and by intermittent streams or plumes of Indian Ocean Water. Ship and satellite data have revealed the presence of numerous large (300- to 400-km diameter) rings of Agulhas Water embedded in the Benguela Current [i.e., *Olson and Evans, 1986; Lutjeharms and van Ballegooyen, 1988; Gordon and Haxby, 1990; Duncombe Rae, 1991*]. These rings form as the western part of the Agulhas Retroreflection pinches off

from the main current. The fate of Agulhas rings and their importance to northward transport of intermediate water are important issues.

Several studies provide estimates of the volume and heat transport carried by these rings from the Indian Ocean to the Atlantic Ocean. On the basis of hydrographic data, *Gordon* [1985] and *Gordon et al.* [1987] suggested a net transfer between 5 to 15 Sv (1 Sv = 10⁶ m³ s⁻¹). *Gordon and Haxby* [1990] used hydrographic data to estimate the transport of Indian Ocean Water by Agulhas rings to be between 10 and 15 Sv. *Byrne et al.* [1995] used maps of surface height anomalies derived from Geosat data to track six Agulhas rings per year and estimated a total value of at least 5 Sv of Indian Ocean Water entering the South Atlantic via those rings. *van Ballegooyen et al.* [1994] observed a total of 14 anticyclonic rings generated by the Agulhas Current over the 2-year period of their study. They estimated a volume flux of Indian Ocean Water warmer than 10°C into the South Atlantic via the Agulhas eddy field of 6.3 Sv and a corresponding heat flux of 0.045 PW.

From 1992 to 1994 the Benguela Sources and Transports Experiment (BEST) [*Garzoli and Gordon, 1996*] studied the flow of the eastern boundary of the South Atlantic Subtropical Gyre. One of the main results of that program was the confirmation that transients, mostly in the form of Agulhas rings, are a major component of the Benguela Current. Observations revealed that at 30°S the Benguela Current transport consisted of a nearly steady flow confined between the South African coast and approximately 4°E (amounting to 10 Sv in the mean) and a more transient flow (3 Sv in the mean) between 4°E and the Walvis Ridge [*Garzoli and Gordon, 1996*]. *Duncombe Rae et al.* [1996] concluded that a minimum of four to six rings of Agulhas origin entered the Cape Basin per year during BEST and were responsible for the transfer of 0.007 PW and 2.6–3.8 Sv between the two basins. *Goñi et al.* [1997] used BEST data and TOPEX/POSEIDON-derived maps of upper layer thickness to estimate that five, four, and six rings were shed from the Agulhas Current during 1993, 1994, and 1995, respectively, with an average of 1 Sv contributed by each to the volume transport of the Benguela Current. *Arhan et al.* [this issue]

¹Atlantic Oceanographic and Meteorological Laboratory, NOAA, Miami, Florida.

²Woods Hole Oceanographic Institution, Woods Hole, Massachusetts.

³Sea Fisheries Research Institute, Cape Town, South Africa.

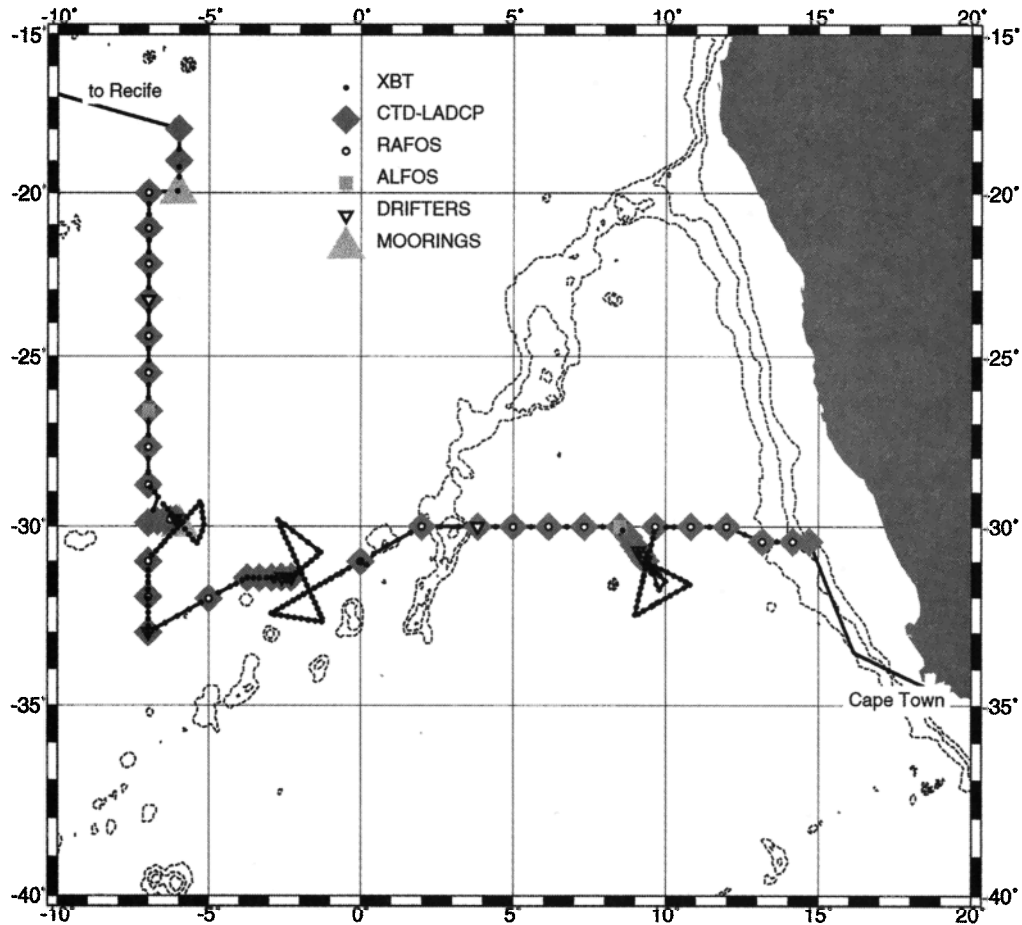


Figure 1. Cruise track and location of the stations occupied during the R/V *Seward Johnson* cruise, September 4–30, 1997. The RAFOS and ALFOS floats will drift for 2 years. Three Agulhas rings were found and surveyed near 31.0°S, 9.4°E; 31.5°S, 2.3°W; and 29.8°S, 6.1°W.

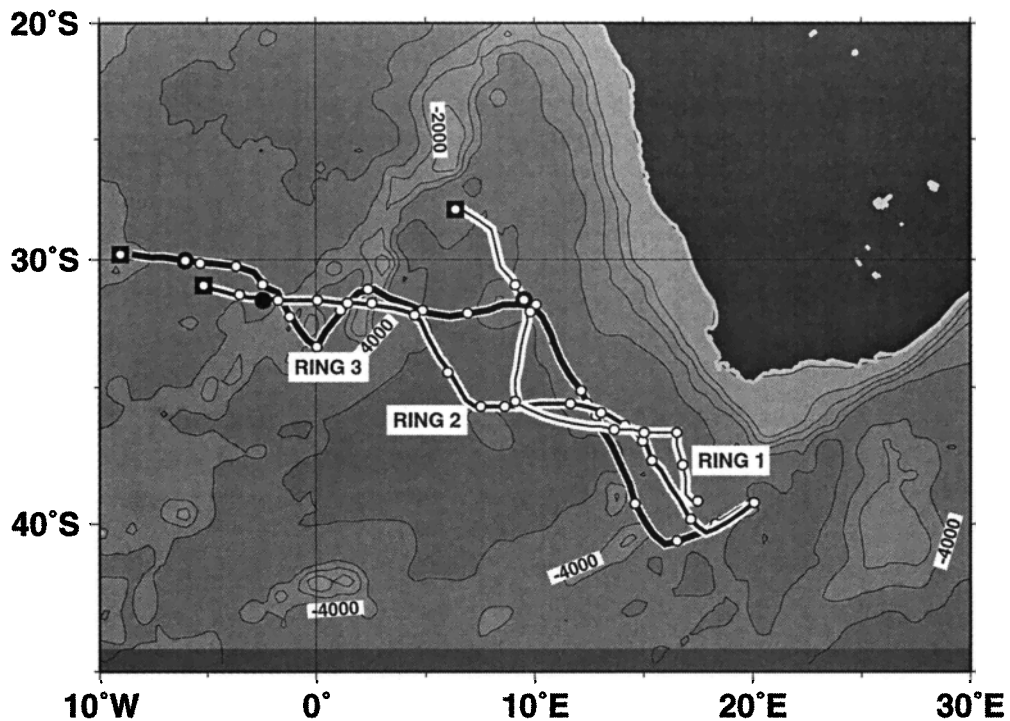


Figure 2. Paths of rings 1, 2, and 3 as revealed from the upper layer thickness maps derived from altimetry. Open circles show the mean location of rings each month. The altimetry-derived ring locations during the cruise are shown with solid circles, and those for November 1997 are shown with solid squares. The spacing between monthly open circles is smaller for rings 2 and 3 near the Walvis Ridge, implying a slower ring speed. Topographic contours are drawn every 1000 m.

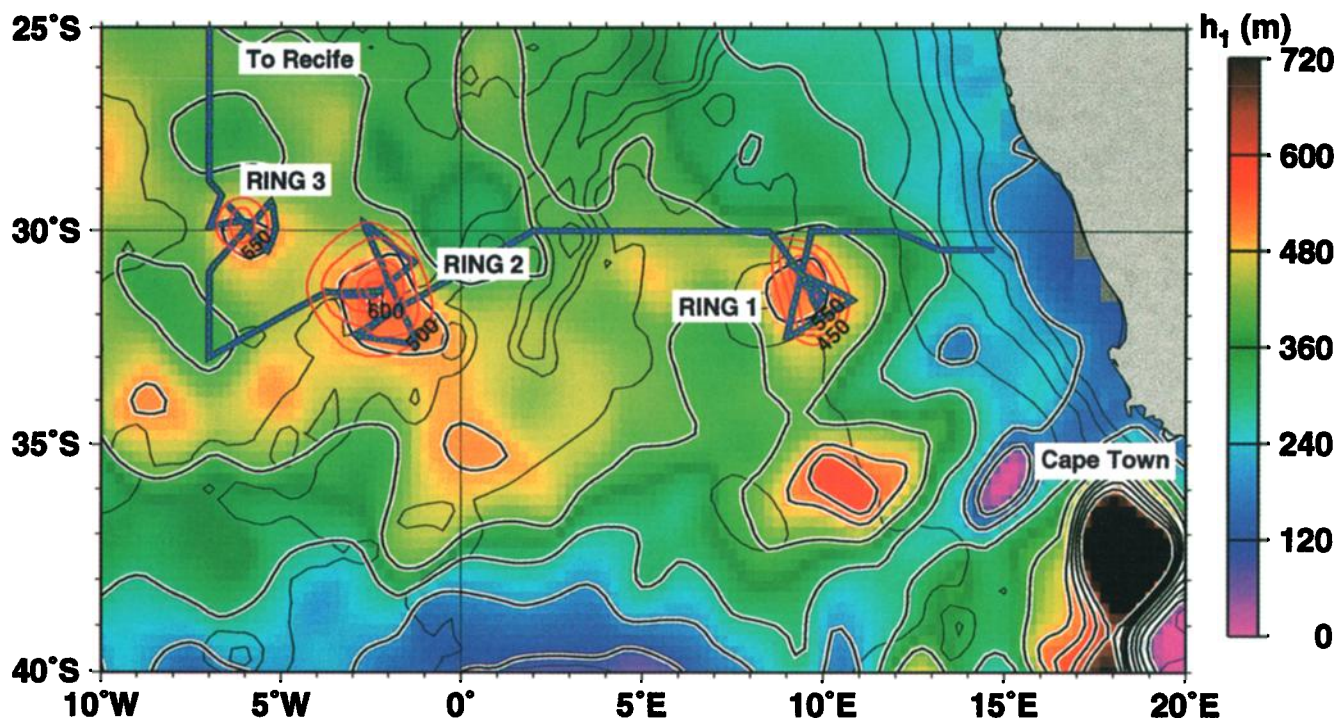


Plate 1. Locations of the three rings as depicted by the altimeter upper layer thickness map corresponding to September 16, 1997. Also shown are the cruise tracks (blue line), hydrography-derived depths (meters) of the 10°C isotherm (red contours), and bathymetry (black contours).

describe three Agulhas rings observed on World Ocean Circulation Experiment (WOCE) hydrographic sections and tracked the rings with altimetry back to their formation. Their rings were inferred to be formed from the retroflection in March 1994 (ring 1) and May 1993 (rings 2 and 3). Estimated ages were 11 months (ring 1) and 21 months (rings 2 and 3).

The present Benguela Current Experiment aims to quantify the flow of intermediate water carried into the South Atlantic by the Benguela-Agulhas system and to track its extension to the northwest with an array of 32 subsurface RAFOS floats deployed near a depth of 700 m. This experiment is part of an international cooperation among the United States, Germany, and South Africa called KAPEX (Cape of Good Hope Experiment) [Boebel *et al.*, 1998], whose main focus is the exchange and advection of water at intermediate depths (700–1000 m) around southern Africa. During KAPEX, more than 100 RAFOS floats are measuring ocean trajectories for the first time in the Agulhas Current, in Agulhas rings that enter the South Atlantic, and in the Benguela Current and its extension. In addition, conductivity-temperature-depth (CTD), expendable bathythermograph (XBT), and velocity profiles are being collected to document the water mass and velocity structure of the Benguela Current, its extension, and several Agulhas rings.

In this paper, results obtained during Agulhas ring surveys performed on the R/V *Seward Johnson* in September 1997 [Roubicek *et al.*, 1998] are presented and discussed. The data consist of XBT surveys, conductivity-temperature-depth-oxygen (CTDO) stations, direct current measurements from a lowered acoustic Doppler current profiler (LADCP) and a hull-mounted ADCP, satellite-tracked surface drifter trajectories, and TOPEX/POSEIDON satellite altimetry measurements. In addition, a total of seven RAFOS floats and six

surface drifters were launched in the rings in order to measure their movement and evolution. This data set is one of the most complete ever obtained of Agulhas rings.

2. September 1997 Cruise

The R/V *Seward Johnson* departed Cape Town, South Africa, on September 4, 1997, and arrived in Recife, Brazil, on September 30, 1997 (Figure 1). The main fieldwork consisted of 44 CTDO-LADCP stations to 2000 m depth or the bottom along the nominal lines 30°S (15°E–7°W) and 7°W (33°S–18°S). The locations of the stations are indicated in Figure 1. XBT surveys were carried out to identify and map three Agulhas rings encountered. The XBT surveys were guided by maps of the depth of the 10°C isotherm derived from TOPEX/POSEIDON altimeter data [Goñi *et al.*, 1997]. The altimetry measured the anomalous height field of the surveyed region and indicated the approximate position of the three rings. The rings were identified and carefully mapped by shipboard measurements. The availability of altimetry enabled the ring survey component of the cruise to be accomplished very efficiently.

3. Rings

Each ring was initially surveyed with XBTs and the hull-mounted ADCP to provide a measure of size and shape. A radial section of five CTDO-LADCP stations was then made in a northwesterly direction from the center to the outer edge of each ring to study the water mass characteristics of the core and the structure of the velocity field. The main thermocline of each ring showed a 200- to 300-m bowl-shaped depression. Plate 1 shows the position of the three rings as depicted by the

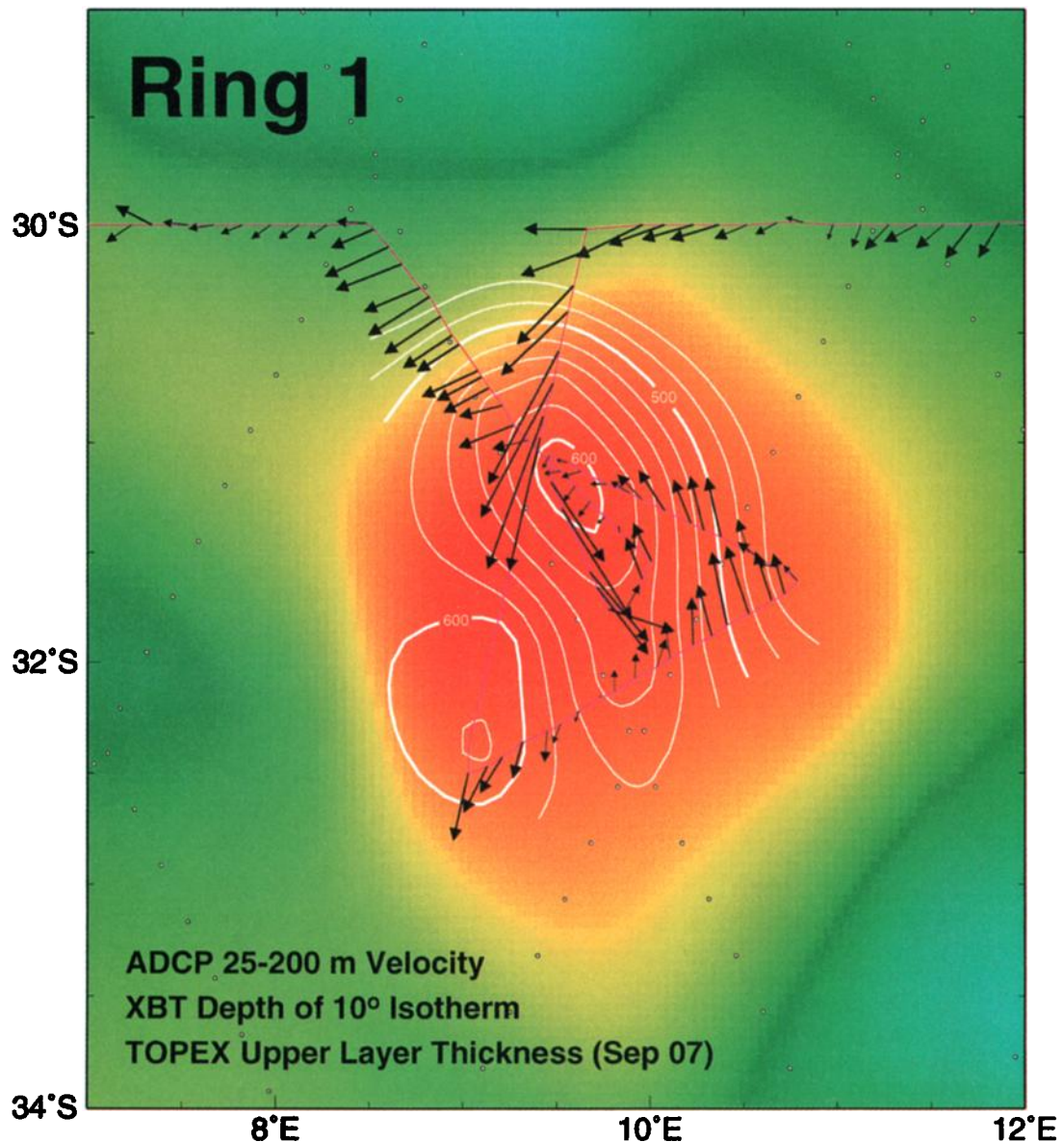


Plate 2. Ring 1. Vectors are acoustic Doppler current profiler (ADCP) upper ocean velocity averaged between 25 and 200 m along the cruise track. The upper layer thickness from TOPEX/POSEIDON altimetry is depicted in the colored background images. Red shades correspond to greater thickness, green shades to lesser thickness. The locations of the TOPEX/POSEIDON data points are indicated by small circles. The 10°C isotherm depth determined from the expendable bathythermograph (XBT) surveys is contoured in white.

altimeter-derived upper layer thickness map corresponding to September 16, 1997 (midcruise), and the hydrography-derived depth of the 10°C isotherm. The agreement between altimetry and hydrography in the location of the rings is remarkable and is a validation of the method used to derive the upper layer thickness of the ocean from the sea surface height observed with the altimeter [Goñi *et al.*, 1997].

Similar upper layer thickness maps were constructed after the cruise, one per day, and used to track these three rings back in time to their origin (see Figure 2). Our analysis reveals that rings 1, 2, and 3 were shed at the retroflection region in February 1997, July 1996, and April 1996, respectively. This suggests that their ages at the time of the cruise were 7, 14, and 17 months, respectively. The computed mean translation speed

values are 9, 8, and 8 cm s^{-1} (or 8, 7, and 7 km d^{-1}) for rings 1, 2, and 3, respectively. These translation speeds fall between previously observed extreme values of 5 and 15 km d^{-1} [Goñi *et al.*, 1997]. Figure 2 also shows that the rings appear to move faster when they are over deeper regions and slower over the shallower areas, such as the Walvis Ridge.

The horizontal structure of the rings, as well as the surface velocities, can be seen in Plates 2, 3, and 4. Ring 1 (Plate 2) was significantly less circular than the other two. We believe this is due to its close proximity to Vema Seamount, which rises up to a depth of 12 m near 31°41'S, 8°20'E. Rings 2 and 3 were relatively close to each other (400 km, two ring diameters) and may have been interacting with each other at the time they were observed.

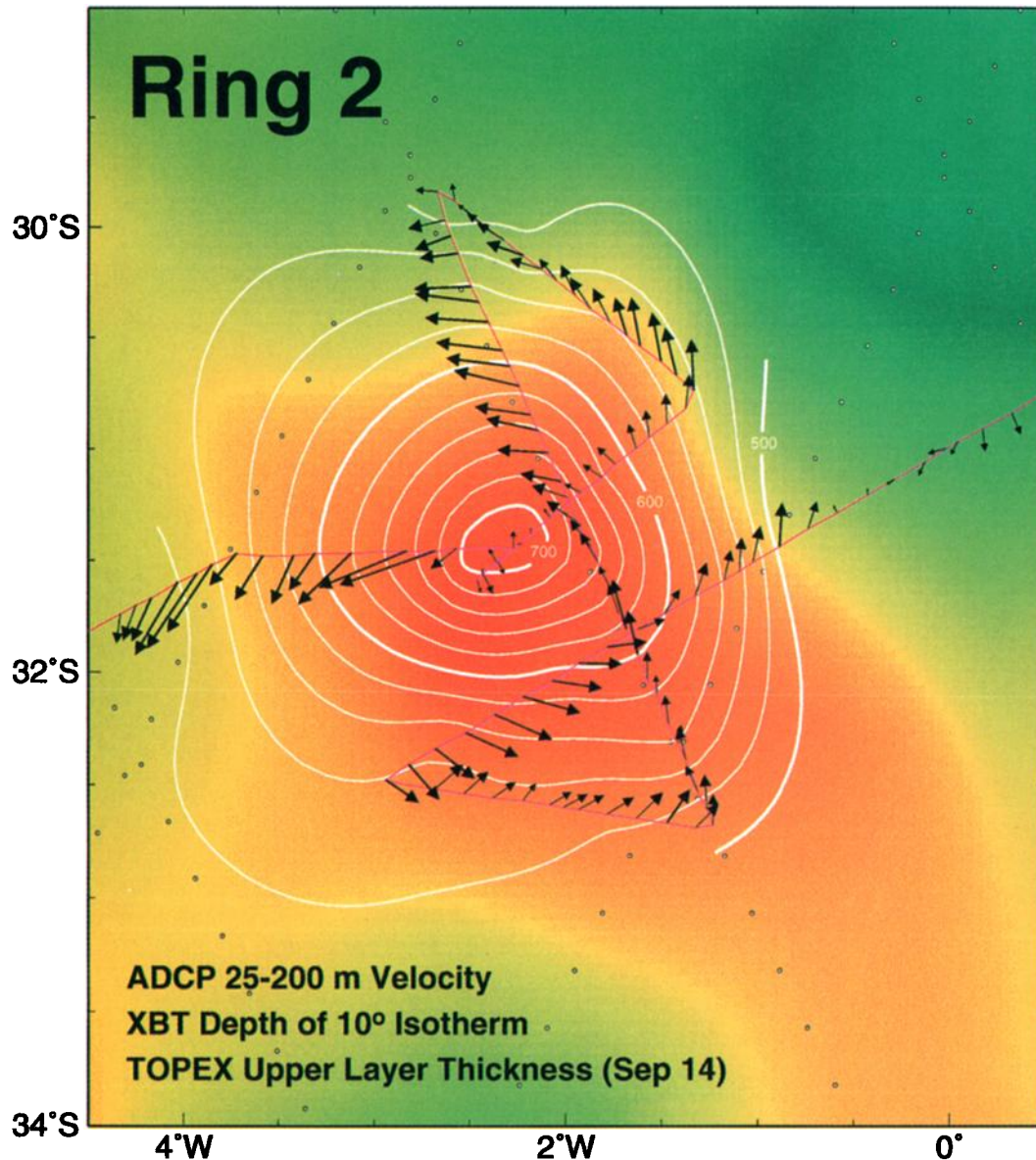


Plate 3. Same as Plate 2, but for ring 2.

The trajectories of satellite-tracked surface drifters launched near the center of each of the three observed rings are shown in Figure 3. The ring trajectories derived from altimetry are also shown for comparison. Three drifters were launched near the center of ring 1. Two of them were immediately ejected from the ring core, possibly owing to deformation experienced by ring 1 during its close encounter with the Vema Seamount. The remaining drifter in ring 1 looped for 1 year. This is the longest time an Agulhas ring has been tracked with drifters. The trajectory in ring 1 showed evidence of a change in translation direction and ring shape as ring 1 approached the Walvis Ridge. Two drifters launched in ring 2 looped simultaneously within the ring for about 120 days before they failed. A single drifter launched in ring 3 was expelled after three or four rotations about the ring center and subsequently drifted westward in the Benguela Current extension. The trajectories followed by the three rings were in the previously identified “ring

corridor” [Garzoli and Gordon, 1996; Goñi et al., 1997], although ring 1 was located on the northern edge of the corridor.

3.1. Ring 1

The altimeter data available just prior to the cruise showed that ring 1 was centered near 32°S, 10°E on August 12–19, 1997. An XBT survey was conducted to determine the size, shape, and precise location of the ring. The survey located ring 1 in the Cape Basin, near Vema Seamount at 31.0°S, 9.4°E on September 9, 1997 or about 1000 km from the Agulhas Retroreflection near 38°S, 17°E. A CTDO/LADCP section was performed along a radial line outward from the ring center. Plate 5 shows a cross section of temperature, salinity, oxygen, and velocity perpendicular to the section along a radial extending northwestward from the center of the ring. The depth of the 10°C isotherm was 630 m at the ring center, compared to 400 m outside the ring (Figure 4). The diameter of the 10°C isotherm

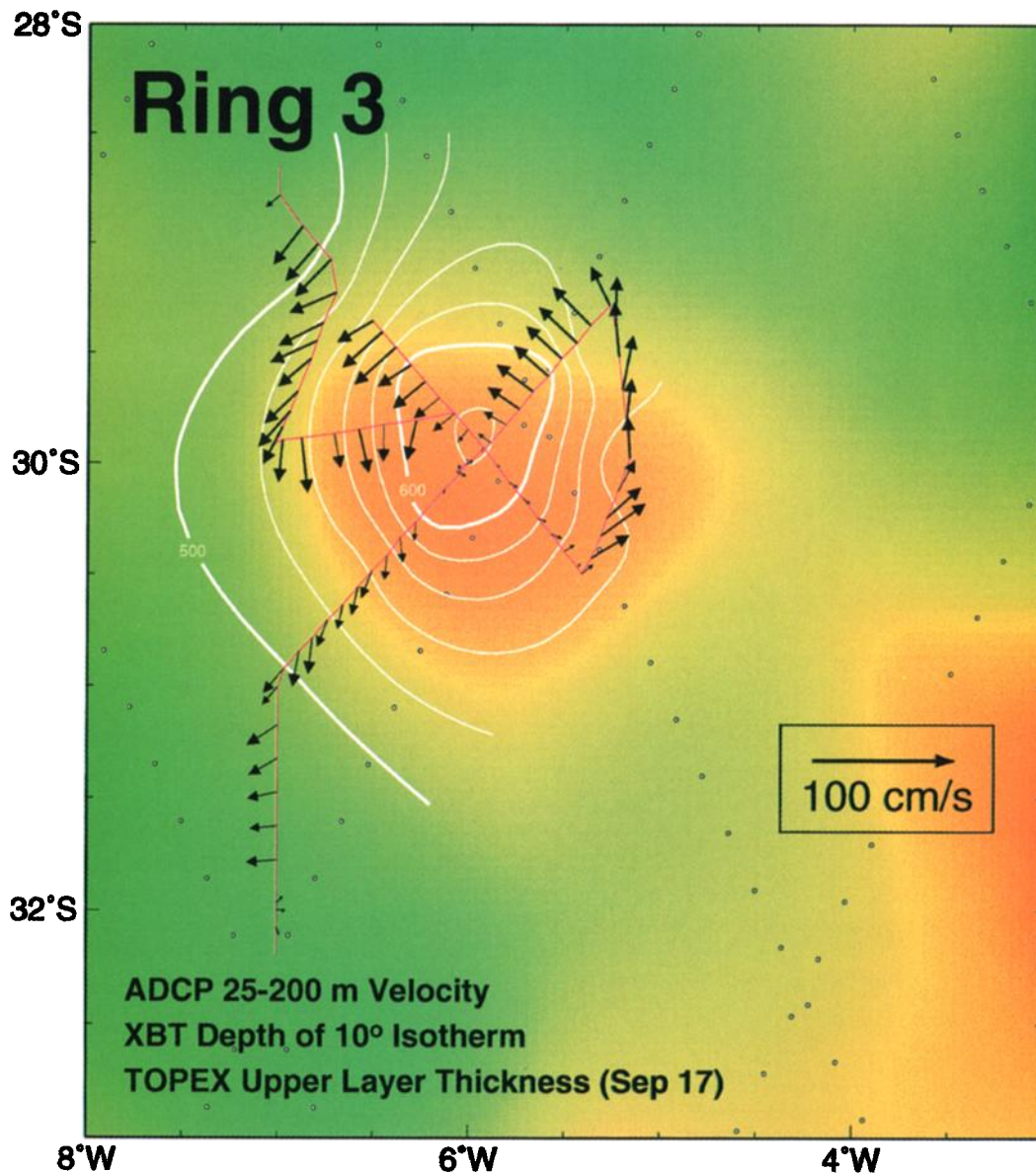


Plate 4. Same as Plate 2, but for ring 3.

at 500 m was approximately 200 km; the ring was elliptical with a major axis oriented northwest-southeast.

Backtracking with TOPEX/POSEIDON altimetry suggests that ring 1 was shed during February 1997 and took 7 months to reach its surveyed position. Ring 1 appears to be a typical Agulhas ring in its first year after shedding, that is to say, with a single thermostad near the surface and a simple, depressed central water thermocline [Duncombe Rae, 1991]. The vertical profile (Plate 5) showed weak vertical gradients of temperature, salinity, and oxygen in a near-surface layer of 200 m in extent with characteristic values of temperature (16.15°C), salinity (35.59), and oxygen (5.62 mL L^{-1}). No other major thermostads occurred within the water column of this ring. The LADCP velocity profiles (Plate 5) indicate maximum near-surface velocities larger than 30 cm s^{-1} . The maximum tangential velocity observed was 36.7 cm s^{-1} . The mean profile of all stations inside the ring (stations 7–12, not shown) shows the tangential velocity decreasing from 23 cm s^{-1} at the surface to

4 cm s^{-1} at 1000 m and then decreasing to the bottom of the profile (2000 m).

In comparison with surrounding water, ring 1 was slightly warmer and carried a small salinity surplus (Figure 4). The entire water column above the Antarctic Intermediate Water, indicated by the salinity minimum, had an oxygen deficit compared to water beyond the ring (Plate 5). This is consistent with the characteristics of the Agulhas Current [Chapman *et al.*, 1987].

3.2. Ring 2

Ring 2 was found near 31.5°S , 2.3°W on September 14, 1997. This ring had translated 1900 km from its presumed formation site near 38°S , 17°E and had already crossed over the Walvis Ridge at the time of our survey. Altimetry showed that ring 2 had left the retroflection during July 1996, 14 months prior to the survey, which gives a mean velocity of 7 km d^{-1} . The

translation speed appeared to decrease over the Walvis Ridge (Figure 2).

Ring 2 was the largest of the three rings encountered: The diameter of 10°C at 500 m was approximately 350 km. The 10°C isotherm reached 732 m at the center, compared to a background depth of around 450 m (Figure 4 and Plate 6). The ring had two near-surface mixed layers with similar characteristics, 60 and 100 m in vertical extent, with temperatures of 16.85°C and 16.65°C , salinities of 35.71 and 35.70, and oxygens of 5.40 and 5.15 mL L^{-1} , respectively. Between 440 and 580 m depth there occurred a thermostad at 12.2°C with salinity between 37.07 and 35.10. This layer had a high oxygen content

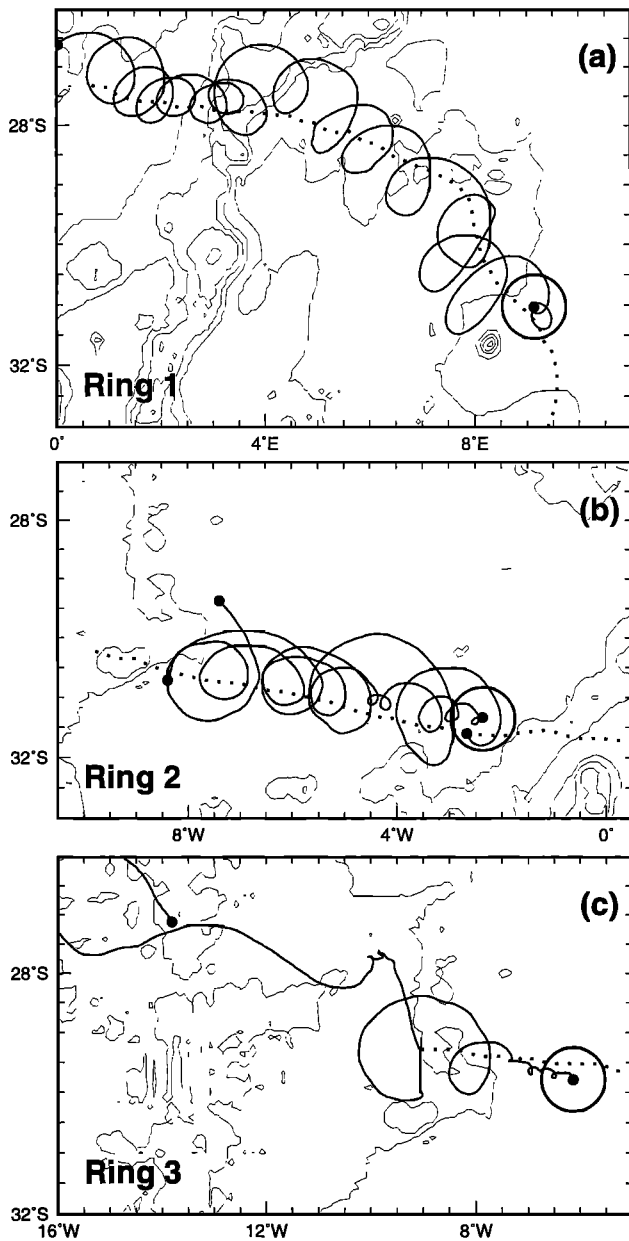


Figure 3. Trajectories of satellite-tracked drifters (solid lines) launched near the center of surveyed rings (a) 1, (b) 2, and (c) 3. Overlapped are the trajectories of the rings from altimetry (dotted lines). The location of the deployment and most recent position of the drifters are indicated by solid circles.

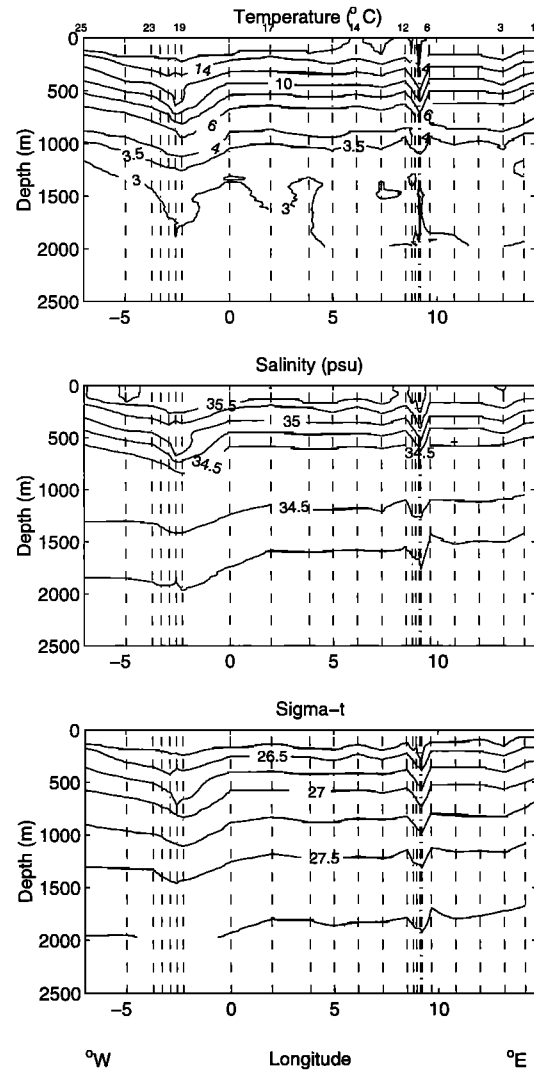


Figure 4. Vertical sections of temperature, salinity, and density versus pressure derived from CTD casts along 30°S (Figure 1). Rings 1 and 2 are indicated by the closely spaced stations and the depression of isotherms near 9°E and 2°W .

(5.35 mL L^{-1}) approaching that of surface waters and was 90% (0.9) saturated. A subsurface velocity maximum (station 19) was observed near 800 m, presumably related dynamically to the depression of the thermocline underneath the deeper well-mixed layer (Plate 6). The mean profile (stations 20–24) has a mean tangential surface velocity of 16.3 cm s^{-1} and a second maximum of 20 cm s^{-1} at 300 m. The velocity decreases to a value of 4 cm s^{-1} at 1000 m and remains constant to 1500 m similar to the mean tangential profile for ring 1.

The hydrographic survey of ring 2 indicates that this ring was different from rings 1 and 3 and unlike most previously observed Agulhas rings. A typical Agulhas ring has a deep thermostad that is more saline, warmer, and lower in oxygen than the surrounding water. In contrast, ring 2 has characteristics between density surfaces 26.5 and 26.7 close to that of the surrounding water, relatively colder, fresher, and more oxygen rich than typical Agulhas rings. In section 5, further analysis of altimetry and a study of the water mass characteristics of ring 2 are presented to determine its origin.

Table 1. Ring Characteristics

Parameter	Ring 1	Ring 2	Ring 3
Depth of 10°C isotherm, m			
from XBT	630	735	625
from altimeter	600	650	600
Maximum tangential velocity, cm s ⁻¹			
from ADCP	50	40	35
from LADCP	37	23	25
Radius of maximum tangential velocity, km			
from ADCP	100	90	95
from LADCP	100	110	100
Mean translation speed, cm s ⁻¹			
from drifters	5.5	6.5	6.3
from altimeter	9	8	8
Translation direction	303	276	287
Rotation period, days	13.1	12.5	N/A
Rossby number	0.07	0.06	0.05

Abbreviations are defined as follows: XBT, expendable bathythermograph; ADCP, acoustic Doppler current profiler (ADCP); LADCP, lowered ADCP; and N/A, not available. Rossby number is defined as V_{\max}/fR_{\max} , where V_{\max} is the maximum tangential velocity and R_{\max} is the radius of maximum tangential velocity.

3.3. Ring 3

Ring 3, the smallest of the rings surveyed, was centered near 29.8°S, 6.1°W on September 17, 1997. This ring was located roughly 400 km northwest of ring 2 and on the extension of the line joining ring 2 and the Agulhas Retroflection region, 2300 km away. Altimetry analysis showed that the ring was shed during April 1996, 17 months prior to the survey. This indicates a mean translation velocity of 7 km d⁻¹. The 10°C isotherm reached 625 m in the ring center as compared to depths around 450 m outside the ring. The diameter of the 10°C isotherm at 500 m was roughly 200 km.

The vertical structure of ring 3 (Plate 7) showed three regions with weak vertical gradients in temperature, salinity, and oxygen. An upper near-surface layer between the surface and 80 m had a temperature of 17.6°C and a salinity of 35.83. The oxygen concentration was 5.35 mL L⁻¹, and the saturation was 1.00. Another near-surface layer occurred between 140 and 195 m depth with a temperature of 15.25°C and a salinity of 35.51. The oxygen concentration was 5.15 mL L⁻¹ at 0.91 saturation. Deeper in the water column, a layer between 340 and 440 m was measured with a temperature of about 14.45°C and salinity of about 35.45. This layer had an oxygen concentration of 5.0 mL L⁻¹ and saturation of 0.88. It is inferred that these layers formed by convection during the winter of 1996. Salinity and temperature are higher in ring 3 than in the surrounding water between the 26.4 and 26.6 density surfaces. Oxygen shows little variation along density surfaces across this ring.

Near-surface velocities of 25 cm s⁻¹ were observed in ring 3 (station 29, Plate 7). A subsurface velocity maximum (38 cm s⁻¹) was observed near 700 m (station 29), presumably related to the depression of the thermocline underneath the subsurface well-mixed layers. The average mean tangential velocity profile has two maxima of 18 cm s⁻¹ from 0 to 100 m and at 650 m. After 1000 m the velocity indicates a similar behavior to rings 1 and 2. This deep mean velocity is in the direction of the translation of the ring and is of the same order of magnitude as the translation velocity obtained from the drifters (section 4).

This could be an indication of the ring moving as a cylinder of water.

4. Geometric and Dynamic Ring Parameters

Fundamental ring geometric and dynamic parameters were calculated for the three rings (Table 1). The depth of the upper layer was calculated from the hydrographic observations and the altimeter-derived sea height anomalies. The maximum tangential velocity and the radius of maximum tangential velocity were determined from smooth radial ADCP and LADCP profiles. The ADCP-measured velocities are consistently higher than the LADCP ones. The translation direction and the rotation period were determined from satellite-tracked surface drifters (except for ring 3; see Figure 3). The mean translation speed was obtained both from the satellite-tracked drifters and the altimeter data.

The size and intensity of the rings can be quantified in terms of ring volume anomaly relative to its surrounding water and ring energy content. Available potential energy, volume anomaly, and heat content anomaly were calculated for each ring.

The volume anomalies of the rings were computed following *Olson and Evans* [1986] and *Duncombe Rae et al.* [1996]:

$$\text{VOL} = \int_A [h_1(r) - h_\infty] dA$$

where $h_1(r)$ is the depth of the ring signature inside the area A and h_∞ is the depth of the thermocline in a region outside of the rings' influence.

Assuming that the ring cross section has a Gaussian shape,

$$\text{VOL} = 2\pi L^2 h_0$$

where L is the radius of maximum velocity and $h_0 = h - h_\infty$ is the difference between the maximum depth of the ring, defined as the region of maximum shear, and h_∞ .

The available potential energy (APE) for each ring was obtained following *Duncombe Rae et al.* [1996]:

$$\text{APE} = \rho g' \pi h_0^2 L^2 / 2$$

where ρ is the mean water density and g' is the mean reduced gravity ($g' = 0.011 \text{ m s}^{-2}$). The heat content of the ring volume anomalies was estimated following *van Ballegooyen et al.* [1994]:

$$Q = \rho C_p \text{VOL} \Delta T$$

where C_p is the specific heat of the seawater, VOL is the volume anomaly computed above, and ΔT is the difference between the temperatures inside and outside the ring. Volume and heat transports are the amount of mass and heat transported by the ring anomalies in a year.

The parameters used to calculate these quantities were derived from the in situ observations. The radius of maximum velocity was determined from the direct measurements (Table 1). The vertical extent of the ring h is obtained from the LADCP-observed tangential velocity profiles. The depths of maximum shear h are 900, 950, and 750 m for rings 1, 2, and 3, respectively (Table 2). For the heat content calculations, ΔT was taken as the difference between the integrated temperature to the depth of the potential density layer corresponding to the depth of maximum shear and the same quantity in a

Table 2. Hydrographic Observations

	L , km	h , m	h_{∞} , m	σ	VOL , $\times 10^{12}$ m ³	T_{VOL} , Sv	Q , $\times 10^{20}$ J	T_q , PW	APE , $\times 10^{15}$ J
Ring 1	100	900	400	27.157	31.4	1	0.88	0.003	43
Ring 2	110	950	400	27.079	41.8	1	1.31	0.004	52
Ring 3	100	750	450	26.987	18.8	0.5	0.77	0.002	15

L is the radius of maximum velocity, h is the depth of maximum shear, h_{∞} is the depth of the unperturbed thermocline outside the ring area, σ is the density of the water at the maximum shear depth, VOL is the volume anomaly of the ring, T_{VOL} is the volume transport (1 Sv = 10^6 m³ s⁻¹), Q is the heat content anomaly, T_q is the heat transport (1 PW = 10^{15} W), and APE is the available potential energy.

region outside the area of influence of the ring. Results are shown in Table 2.

According to Table 2, the amount of mass entering the Atlantic and carried by the rings is 1, 2, and 0.5 Sv for rings 1, 2, and 3, respectively. On the basis of previous estimates of the number of rings shed at the retroflection (four to six per year) and a mean volume transport of 0.8 Sv per ring, the contribution of the rings' transport to the interocean exchange of water ranges from 3 to 5 Sv. The heat transported by rings 1, 2, and 3 is 0.003, 0.004, and 0.002 PW, respectively. These transport estimates are to be considered a lower limit because of the location at which the rings were surveyed and the time elapsed after they were shed from the retroflection, more than 1 year in the last two cases. A rough estimate from *Byrne et al.* [1995] determined that at least 50% of the sea surface height anomaly has disappeared at these distances from the shedding area. In addition, after more than a year, most of the heat transported by the rings may have been lost. As much as twice these values (6 to 10 Sv and 0.006 PW per year) are more reasonable estimates of the contributions of the rings to the interocean exchange of mass and heat.

The available potential energy of the rings (Table 2) is 43, 52, and 15×10^{15} J for rings 1, 2, and 3, respectively. Previous estimates of rings in the region [*van Ballegooyen et al.*, 1994; *Duncombe Rae et al.*, 1996; *Goñi et al.*, 1997] ranged from 1 to 71×10^{15} J with an average of 24×10^{15} J.

It is not always possible to calculate these parameters from in situ observations. The altimeter data provide an independent way in which the sea height anomaly along with climatological data can provide a good proxy to estimate these parameters. In what follows the same variables were calculated from the altimeter-derived sea height anomaly field, which was used to estimate the depth of the 10°C isotherm. Here h_0 is obtained as the difference between the maximum depth of the upper layer (in this case represented by the depth of the 10°C isotherm) in the ring and in a region outside the ring influence (h_{∞}) at the time of the hydrographic observations. L is the radius of maximum velocity, which is given by the length scale of the Gaussian fit of the altimeter-derived upper layer thickness section of the ring. The maximum altimeter-derived upper

layer thickness depths at the time of the hydrographic observations were 605, 655, and 600 for rings 1, 2, and 3, respectively (Table 1). These estimates are slightly smaller than the observed XBT values since the altimeter ground tracks were not probably crossing the center of the rings during the XBT observations. The volume transport anomalies of each ring entering the South Atlantic were estimated by dividing the volume anomaly by the number of seconds in a year, with values of 0.4, 0.4, and 0.3 Sv for rings 1–3, respectively. The available potential energy of the rings was computed from the altimeter-derived sea height anomaly data [*Goñi et al.*, 1997] to be 10, 17, and 3×10^{15} J for rings 1, 2, and 3, respectively. The heat content with respect to the 10°C isotherm, Q , was computed [*Shay et al.*, 1999] by considering ΔT as the difference between the 10°C isotherm and temperature of the surrounding waters, taken here as 15°C, to compare with previous estimates of *van Ballegooyen et al.* [1994]. In this case, h is the difference between the depth of the 10°C and 15°C isotherms. The heat transport values calculated for the three rings are 0.005, 0.006, and 0.003 PW for rings 1, 2, and 3, respectively. It is interesting to note that the calculations from the satellite underestimate the volume transport and APE by half and that the heat content is larger. The latest is due to the method used that assumes always a difference of temperature of 5°C between the interior of the rings and the surrounding waters. The estimates of all the altimeter-derived parameters are shown in Table 3.

The radial distributions of the 10°C isotherm depth and the tangential (swirl) velocity were determined from the shipboard XBT and ADCP surveys (Figures 5 and 6). The scatter in the individual depth and velocity observations is due in part to ring motion (both translation and rotation) during the 36- to 72-hour ring surveys. Noncircular ring geometry (particularly evident in ring 1) also contributed to the observed scatter. It is interesting to note (Figure 5) that while the maximum depth of the 10°C isotherm is greatest by almost 100 m in ring 2, the net change in isotherm depth across each ring is similar (about 200 m). The decrease in maximum swirl velocity from ring 1 to ring 3 (Figure 6) is consistent with the time and distance each ring has traveled from the Agulhas Retroflection.

Table 3. Altimeter Observations

	L , km	h_1 , m	h_{∞} , m	VOL , $\times 10^{12}$ m ³	T_{VOL} , Sv	Q , $\times 10^{20}$ J	T_q , PW	APE , $\times 10^{15}$ J
Ring 1	100	605	400	13	0.4	1.5	0.005	10
Ring 2	90	655	400	13	0.4	1.7	0.006	17
Ring 3	95	600	500	11	0.3	0.9	0.003	3

L is the length scale of the ring obtained from a Gaussian fit of the 10°C isotherm; h_1 is the maximum depth of the 10°C isotherm in the center of the ring; h_{∞} is depth far from the ring; VOL , T_{VOL} , Q , T_q , and APE are as listed in Table 2.

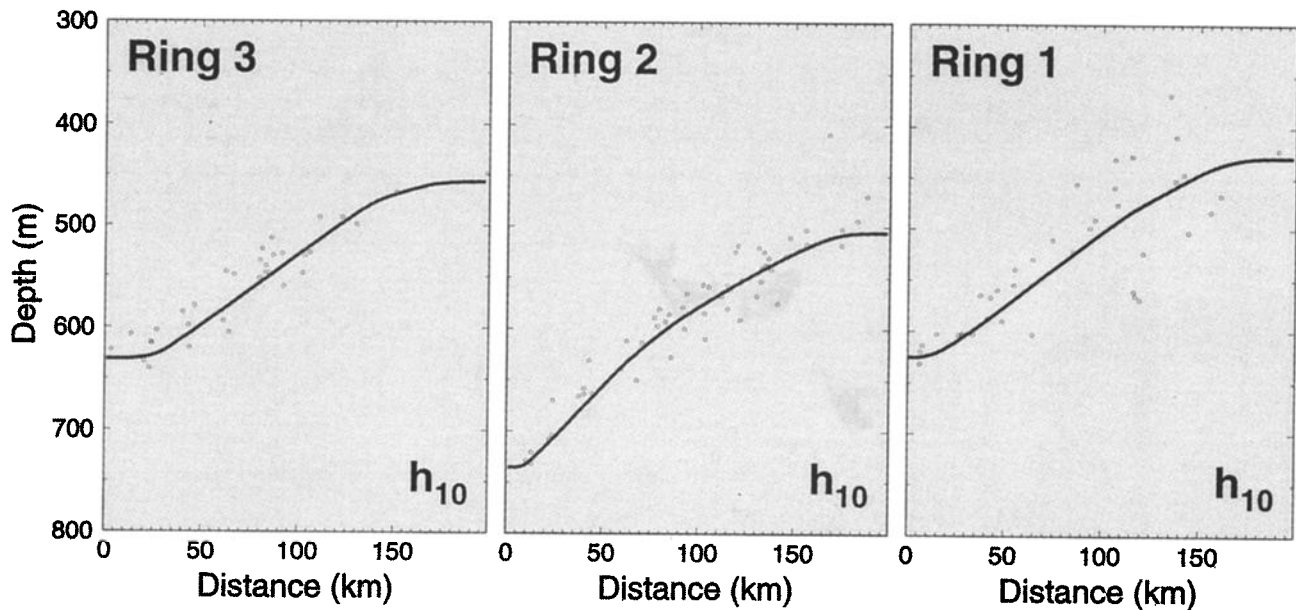


Figure 5. Depth of the 10°C isotherm determined from the shipboard XBT and ADCP surveys as a function of the distance from the center of the rings.

5. Origin of the Rings

Ring 1 showed the typical profile of a young Agulhas retroflection ring during the first year after shedding [Duncombe Rae, 1991]. There is a reasonably well defined upper thermostat, and the main thermocline is unbroken by additional thermostads. Similarly, the water mass characteristics of ring 3 suggest that its structure can be explained in terms of successive atmosphere-driven heating/mixing and cooling/mixing events over the 17 months since leaving the vicinity of the retroflection. The property characteristics of rings 1 and 3 also appear to be usual for Agulhas rings. Salinity and temperature

are high and oxygen is low relative to the surrounding South Atlantic Water.

The hydrography of ring 2, however, appears to be atypical. The structurally anomalous portion of the water column of this ring lies about the 26.61 isopycnal. At this density level the temperature and salinity are not noticeably distinct from the surrounding water. Only the oxygen concentration (5.4 mL L^{-1}) at this level appears different from the surrounding water and indicates recent contact with the atmosphere (O_2 saturation ~ 0.9). The 26.61 isopycnal approaches the surface in the Subtropical Front around 40°S in the South Atlantic Ocean

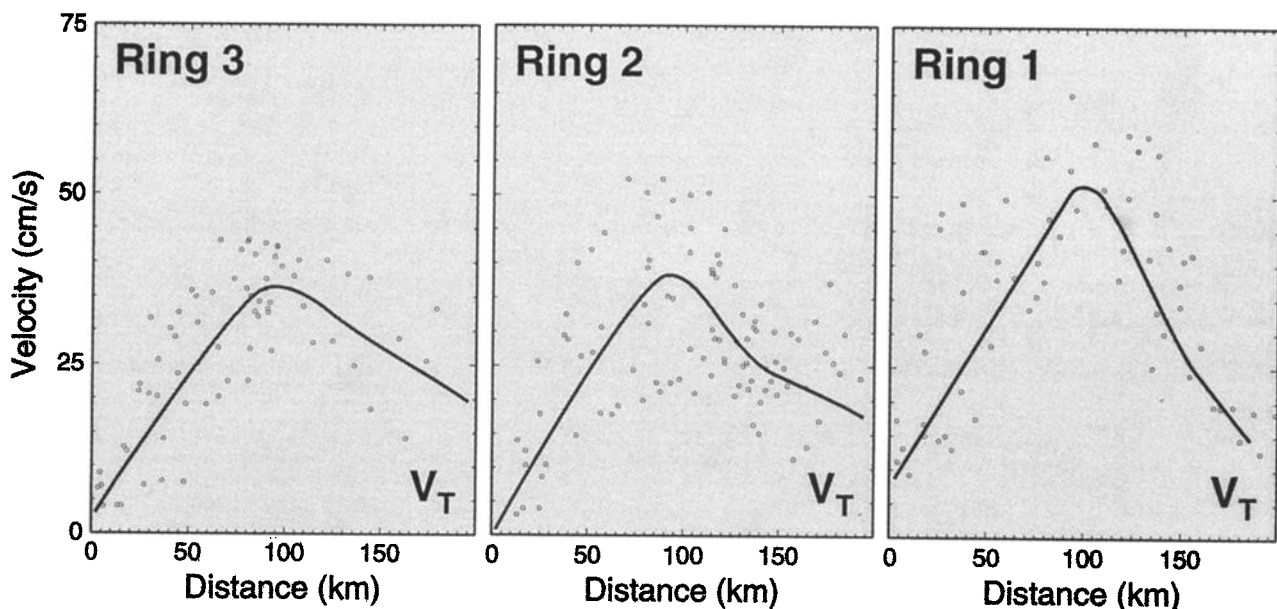


Figure 6. Tangential (swirl) velocity determined from the shipboard XBT and ADCP surveys as a function of the distance from the center of the rings.

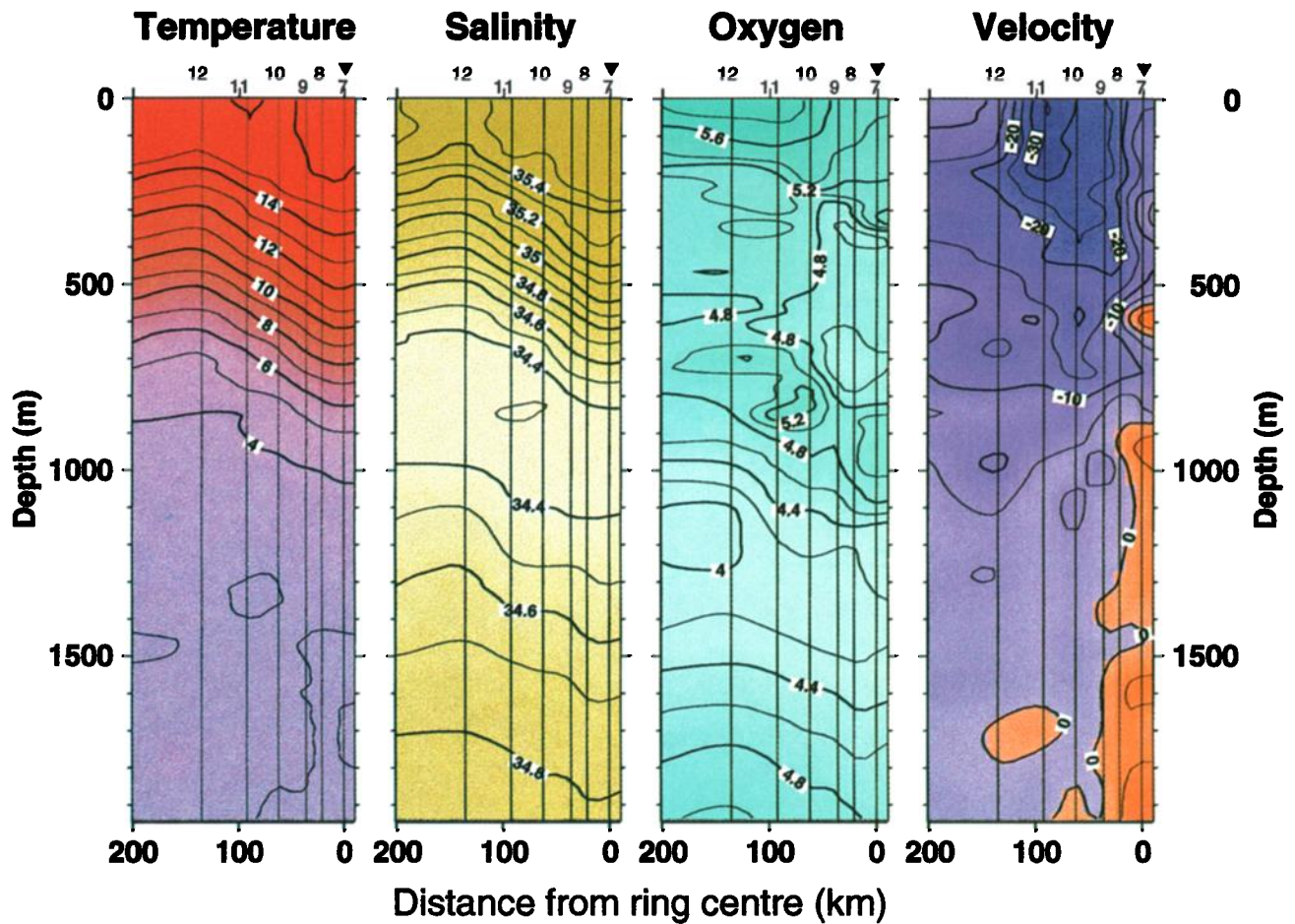


Plate 5. Vertical sections of temperature ($^{\circ}\text{C}$), salinity (psu), oxygen (mL L^{-1}), and cross-section velocity versus pressure for ring 1 derived from conductivity-temperature-oxygen/lowered ADCP (CTDO/LADCP) casts. The radial section is northwestward from the center of the ring. The center is indicated with an arrowhead. Approximate distance from ring center is indicated on the horizontal axis.

(Plate 8). The 26.61 isopycnal is close to the density of Subantarctic Mode Water [McCartney, 1977]. Although there is some evidence of water on this density level with oxygen saturation values near 0.9 in the Indian Ocean, the density surface generally has oxygen concentrations below 5 mL L^{-1} in the Indian Ocean. With the exception of the retroflection, the Agulhas Current and recirculation are particularly depleted in oxygen. However, high saturation and concentrations of oxygen do occur on this density surface in the South Atlantic. This observation accomplishes two objectives: it rules out an Agulhas Current or Indian Ocean origin of the anomalous thermostad and indicates a South Atlantic origin.

The following three scenarios can be envisaged that account for the structure of ring 2:

1. The ring was formed completely at the Agulhas Retroflection with the anomalous thermostad in some manner created by the incorporation of Subantarctic Water during the process of eddy shedding when water with low salinity, low temperature and high oxygen was drawn between the retroflection and the newly formed eddy [Lutjeharms and van Ballegooyen, 1988].

2. The ring formed normally at the retroflection and later incorporated a lens of water from the Subtropical Front (STF) by coalescing with another eddy. Coalescence of eddies has

been observed in the field in at least two prior studies by Cresswell [1982] and Schultz Tokos *et al.* [1994]. It has also been modeled in the laboratory, under various conditions of eddy densities, vertical extent, and horizontal spacing [Nof and Simmons, 1987; Griffiths and Hopfinger, 1987].

3. The ring may not be of Agulhas origin. Given that prior studies have suggested a Brazil Current origin for some rings encountered in the southeastern Atlantic [Smythe-Wright *et al.*, 1996; Duncombe Rae *et al.*, 1996], it is possible that ring 2 described here may have been shed from the Brazil Malvinas Confluence.

The origin of the water in this ring must remain undetermined, with coalescence with an eddy from the STF the more likely source, without totally discounting the others as possible explanations. Ring 2 was readily tracked back to the Agulhas Retroflection in the altimetry and was observed to spend an appreciable amount of time south of the STF, allowing ample opportunity for incorporation of an eddy from the STF and suggesting that scenario 3 may be discarded.

Arhan *et al.* [this issue] observed, in one of the three rings that they analyzed, a thermostad of 11.6°C (their ring 1). It was also associated with somewhat anomalous water properties, lower in salinity and higher in O_2 , compared to more usual Agulhas rings. Their ring was also inferred to have formed

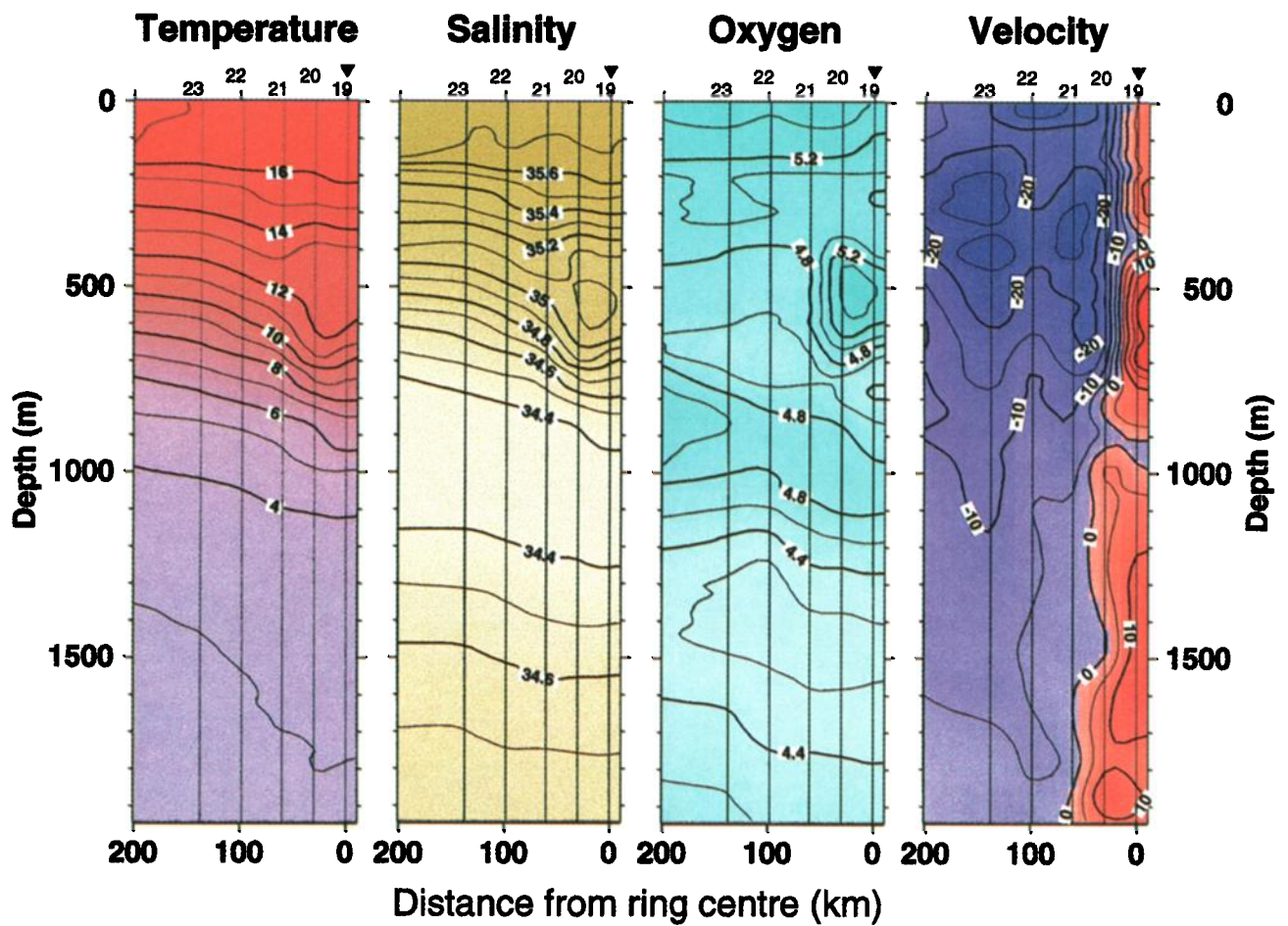


Plate 6. Same as Plate 5, but for ring 2. The radial section is westward from the center of the ring. The center is indicated with an arrowhead. Approximate distance from ring center is indicated on the horizontal axis.

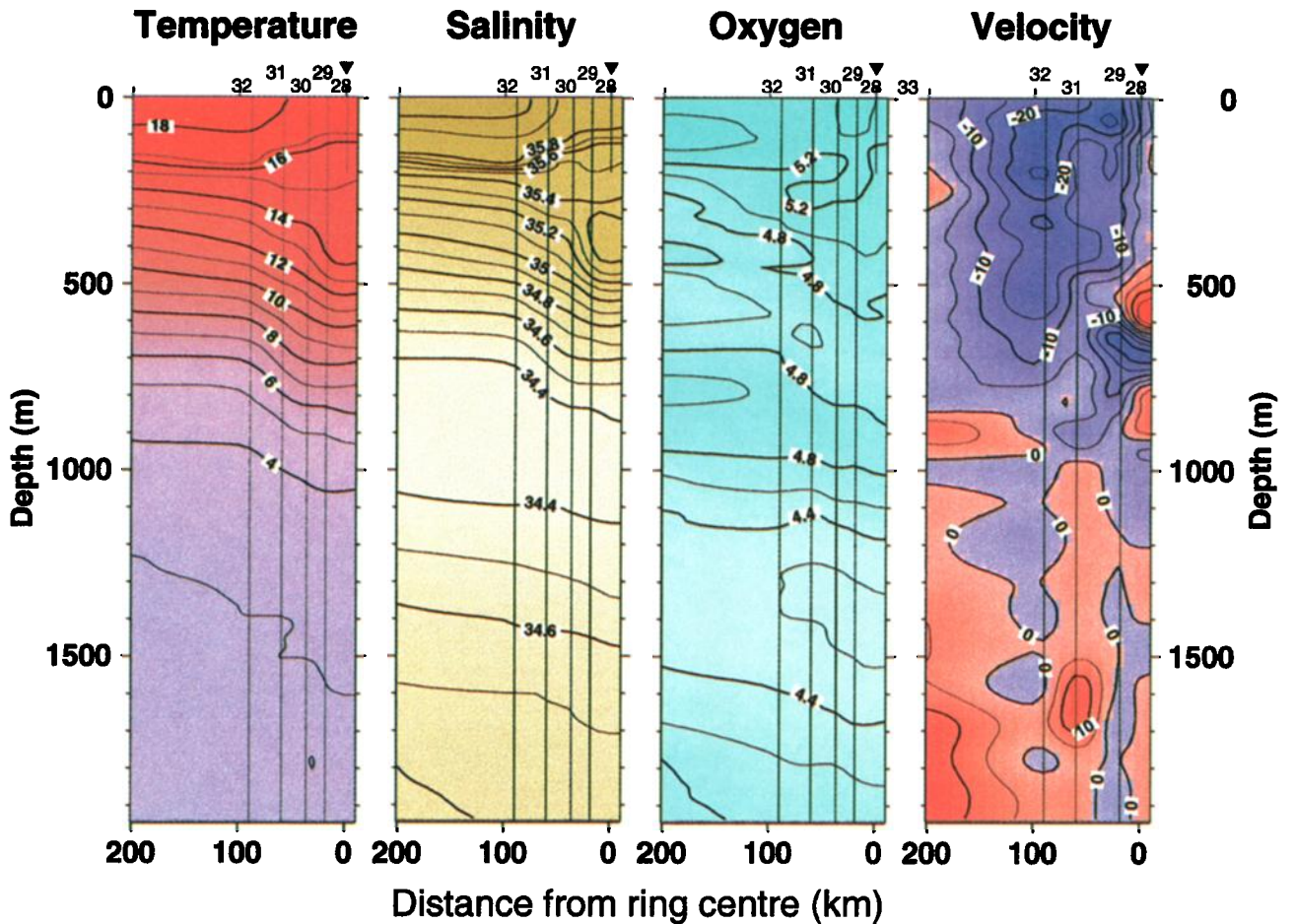


Plate 7. Same as Plate 5, but for ring 3. The radial section is westward from the center of the ring. The center is indicated with an arrowhead. Approximate distance from ring center is indicated on the horizontal axis.

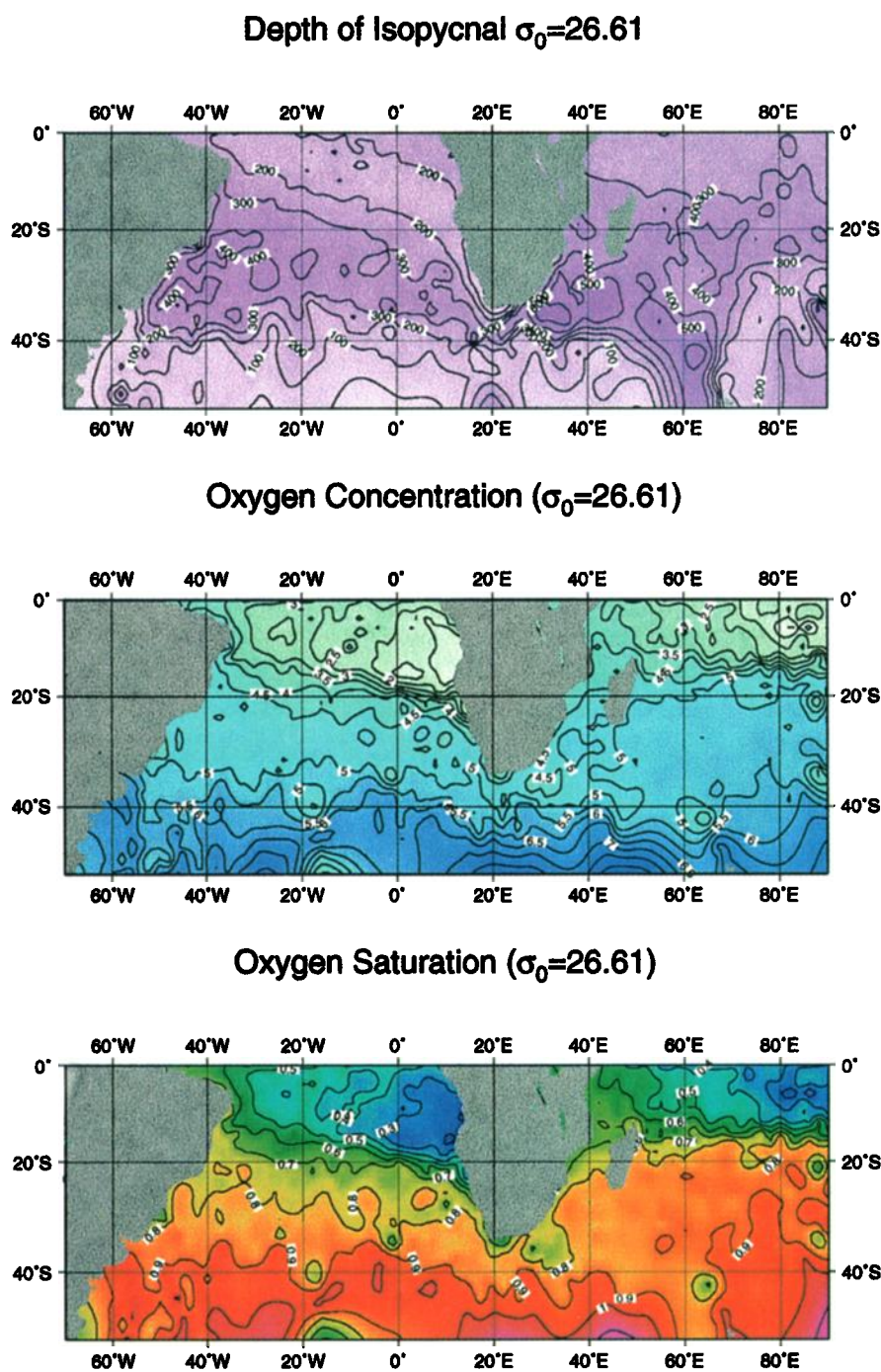


Plate 8. Distribution of properties on the 26.61 kg m^{-3} density surface in the South Indian and South Atlantic Oceans. Data from NODC database include (top) depth of the density surface, (middle) oxygen concentration (mL L^{-1}) on the density surface, and (bottom) oxygen saturation on the density surface.

from the Agulhas Retroflection. Arhan et al. suggest that the 11.6°C thermostat in their ring 1 was formed by intense convective modification of Agulhas ring water during a winter spent south of 42°S . The surface water above the core was explained as being colder, fresher, and more oxygenated Subantarctic Surface Water (SAASW) that had become entrained by the ring as it transited through the Subantarctic Zone and subducted beneath the SAASW. We attempted to model the formation of the 12.2°C cold thermostat in our ring 2 but

concluded that both extreme cooling and much higher than usual precipitation throughout the period since shedding were required. The additional capping of the cold thermostat and the translation of ring 2 across the Walvis Ridge, where we found it, would require even greater cooling and precipitation rates. The presence of water in the nearby Subtropical Front and Subantarctic Zone with the required characteristics of low temperature and low salinity led us to seek a mechanism that could incorporate this water into the ring core. We suggest the

merging of ring 2 and an eddy of Subtropical Front water accomplished this without the need for extreme cooling and precipitation. That two out of the six observed rings contained these cold thermostads suggests that they are more common than previously realized. It must be left for future work to document the mechanism(s) that caused these cold thermostads.

6. Summary and Discussion

Rings shed from the Agulhas Current and carried into the Atlantic as transient components of the Benguela Current are important contributors to interocean heat, salt, and mass transports. The three rings sampled during September 1997 as part of the Benguela Current Experiment add new insight to the origins and physical properties of these energetic features. The rings were measured by a combination of techniques and were backtracked to their formation region with altimetry. The three rings share some common characteristics but also have some significant structural differences. Within each ring the maximum swirl velocity was located at a radius of approximately 100 km. The magnitude of this maximum velocity appeared to decrease roughly proportional to the inferred ages of the rings.

Ring 1 had characteristics typical of Agulhas rings in their first year after shedding [Duncombe Rae, 1991]. The vertical structure of ring 3 can be explained in terms of successive atmosphere-driven heating/mixing and cooling/mixing cycles during the ring's 17-month life.

Ring 2 had embedded into its main core at depths from 440 to 580 m a thermostad of low-temperature (12.2°C), low-salinity (35.07 to 35.10), and high-oxygen concentration. Thermostads of temperatures between 13° and 14°C have been previously observed in these rings. Rings with thermostads between 13° and 14°C and saltier than Agulhas rings have been previously identified as Brazil rings [Smythe-Wright et al., 1996; Duncombe Rae et al., 1996]. The oxygen concentration and saturation within the anomalous thermostad of ring 2 are also different from those observed in Agulhas rings. In this case, three possible sources for the thermostad were examined: vortex stretching during shedding, merging with water from south of the STF, or incorporation of bottom water from the nearby Agulhas Bank. The origin was not resolved conclusively. High saturation and concentrations of oxygen such as found in ring 2 are observed in the South Atlantic. The analysis presented leads to the conclusion that ring 2 is of Agulhas origin and later incorporated a lens of water from the Subtropical Front by coalescing with another eddy. Further understanding of how these rings translate into the interior and their ultimate role in the meridional overturning circulation will be possible once the RAFOS floats deployed in their cores end their mission and provide further data.

Acknowledgments. The scientific party wishes to acknowledge the invaluable support of Captain Vince Seiler and the crew of the R/V *Seward Johnson*, who helped make the cruise a success. The authors wish to acknowledge the scientific collaboration of the members of KAPEX, O. Boebel, J. Lutjeharms, T. Rossby, and W. Zenk, and their helpful comments during the planning stage of this experiment. We especially thank O. Boebel and W. Zenk for deploying one of the U.S. sound sources, which enabled us to spend more time on the ring survey. We are very grateful to Doug Wilson and Ryan Smith (NOAA AOML) for their help in reprocessing the LADCP data and to Warren Krug for his support with the XBT software. Near-real-time altimeter data were provided by Robert Cheney (NOAA/NODC). M. Arhan, H. Mercier, and J. R. E. Lutjeharms generously gave us a preprint of their

paper, which also describes three Agulhas rings. Gail Derr and Veta Green prepared the manuscript for publication. This program was funded by a grant from the National Science Foundation, OCE95-28574, and received additional support from NOAA/AOML/PhOD.

References

- Arhan, M., H. Mercier, and J. R. E. Lutjeharms, The disparate evolution of three Agulhas rings in the South Atlantic Ocean, *J. Geophys. Res.*, this issue.
- Boebel, O., C. M. Duncombe Rae, S. L. Garzoli, J. R. E. Lutjeharms, P. L. Richardson, T. Rossby, C. Schmid, and W. Zenk, KAPEX: Observing the intermediate flow at the tip of Africa, *Eos Trans. AGU*, 79, 1, 7, and 8, 1998.
- Broecker, W. S., The great ocean conveyor, *Oceanography*, 4(2), 79–89, 1991.
- Byrne, D. A., A. L. Gordon, and W. F. Haxby, Agulhas eddies: A synoptic view using GEOSAT ERM data, *J. Phys. Oceanogr.*, 25, 902–917, 1995.
- Chapman, P., C. M. Duncombe Rae, and B. R. Allanson, Nutrients, chlorophyll, and oxygen relationships in the surface layers at the Agulhas Retroflection, *Deep Sea Res., Part A*, 34(8), 1399–1416, 1987.
- Cresswell, L. G. R., The coalescence of two east Australian Current warm-core eddies, *Science*, 215, 161–164, 1982.
- Duncombe Rae, C. M., Agulhas Retroflection rings in the South Atlantic Ocean: An overview, *S. Afr. J. Mar. Sci.*, 11, 327–344, 1991.
- Duncombe Rae, C. M., S. L. Garzoli, and A. L. Gordon, The eddy field of the southeast Atlantic Ocean: A statistical census from the Benguela Sources and Transports Project, *J. Geophys. Res.*, 101, 11,949–11,964, 1996.
- Garzoli, S. L., and A. L. Gordon, Origins and variability of the Benguela Current, *J. Geophys. Res.*, 101, 987–906, 1996.
- Goñi, G. J., S. L. Garzoli, A. J. Roubicek, D. B. Olson, and O. B. Brown, Agulhas ring dynamics from TOPEX/POSEIDON satellite altimeter data, *J. Mar. Res.*, 55(5), 861–883, 1997.
- Gordon, A. L., Indian-Atlantic transfer of thermocline water at the Agulhas Retroflection, *Sciences N. Y.*, 227(4690), 1030–1033, 1985.
- Gordon, A. L., and W. F. Haxby, Agulhas eddies invade the South Atlantic: Evidence from Geosat altimeter and shipboard conductivity-temperature-depth survey, *J. Geophys. Res.*, 95, 3117–3125, 1990.
- Gordon, A. L., J. R. E. Lutjeharms, and M. L. Grundlingh, Stratification and circulation at the Agulhas Retroflection, *Deep Sea Res., Part A*, 34, 565–599, 1987.
- Gordon, A. L., R. F. Weiss, W. M. Smethie, and M. J. Warner, Thermocline and Intermediate Water communication between the South Atlantic and Indian Oceans, *J. Geophys. Res.*, 97, 7223–7240, 1992.
- Griffiths, R. W., and E. J. Hopfinger, Coalescing of geostrophic vortices, *J. Fluid Mech.*, 178, 73–97, 1987.
- Lutjeharms, J. R. E., and R. C. van Ballegooyen, The retroflection of the Agulhas Current, *J. Phys. Oceanogr.*, 18, 1570–1583, 1988.
- McCartney, M. S., Subantarctic Mode Water, in *A Voyage of Discovery, George Deacon: 70th Anniversary Volume*, edited by M. Angel, pp. 103–119, Pergamon, Tarrytown, N. Y., 1977.
- Nof, D., and L. Simmons, Laboratory experiments in the merging of nonlinear anticyclonic eddies, *J. Phys. Oceanogr.*, 17, 343–357, 1987.
- Olson, D. B., Rings in the ocean, *Annu. Rev. Earth Planet. Sci.*, 19, 133–183, 1991.
- Olson, D. B., and R. H. Evans, Rings of the Agulhas Current, *Deep Sea Res., Part A*, 33, 27–42, 1986.
- Peterson, R. G., and L. Stramma, Upper-circulation in the South Atlantic Ocean, *Prog. Oceanogr.*, 26, 1–73, 1991.
- Roubicek, A. J., S. L. Garzoli, P. L. Richardson, C. M. Duncombe Rae, and D. M. Fratantoni, Benguela Current Experiment, R/V *Seward Johnson* Cruise SJ9705, *NOAA Data Rep., ERL AOML-33*, 215 pp., Atlantic Oceanogr. and Meteorol. Lab., Miami, Fla., 1998.
- Saunders, P. M., and B. A. King, Oceanic fluxes on the WOCE A11 section, *J. Phys. Oceanogr.*, 25, 1942–1958, 1995.
- Schultz Tokos, K. L., H.-H. Hinrichsen, and W. Zenk, Merging and migration of two eddies, *J. Phys. Oceanogr.*, 24, 2129–2141, 1994.
- Shay, L. K., G. J. Goni, and P. G. Black, Effects of a warm oceanic feature on Hurricane Opal, *Mon. Weather Rev.*, in press, 1999.
- Smythe-Wright, D., A. L. Gordon, P. Chapman, and M. S. Jones, CAC-113 shows Brazil eddy crossing the South Atlantic to the Agulhas Retroflection region, *J. Geophys. Res.*, 101, 885–895, 1996.

van Ballegooyen, R. C., M. L. Grundlingh, and J. R. E. Lutjeharms, Eddy fluxes of heat and salt from the southwest Indian Ocean into the southeast Atlantic Ocean: A case study, *J. Geophys. Res.*, *99*, 14,053–14,070, 1994.

C. M. Duncombe Rae, Sea Fisheries Research Institute, P. Bag X2, Rogge Bay, 8012 Cape Town, South Africa.
D. M. Fratantoni and P. L. Richardson, Woods Hole Oceanographic

Institution, Woods Hole, MA 02543.

S. L. Garzoli, G. J. Goñi, and A. J. Roubicek, Atlantic Oceanographic and Meteorological Laboratory, NOAA, 4301 Rickenbacher Causeway, Miami, FL 33149. (garzoli@aoml.noaa.gov)

(Received April 17, 1998; revised February 1, 1999;
accepted February 25, 1999.)